

CHROM. 22 939

## **Preparative high-performance liquid chromatography based on reversed-phase gradient elution**

### **Optimum experimental conditions for heavily overloaded separation**

L. R. SNYDER\* and J. W. DOLAN

*LC Resources Inc., 3182C Old Tunnel Road, Lafayette, CA 94549 (U.S.A.)*

and

G. B. COX<sup>a</sup>

*Medical Products Department, E. I. Du Pont de Nemours and Co., Wilmington, DE 19898 (U.S.A.)*

(First received August 2nd, 1990; revised manuscript received September 25th, 1990)

---

#### **ABSTRACT**

Computer simulations based on the Craig distribution model have been used to examine how separation varies with experimental conditions for the case of heavily overloaded (overlapping bands) gradient elution. A close similarity is noted between these gradient separations and "corresponding" isocratic runs (where isocratic capacity factors  $k'$  are equal to gradient capacity factors  $\bar{k}$ ). The present discussion assumes reversed-phase chromatography, although similar conclusions would result for other chromatographic methods (e.g., ion exchange). Attention was also given to the case of sample components having different dependencies of retention on mobile phase composition (different  $S$  values). The special behavior of such samples can be understood in terms of changes in the separation factor  $\alpha$  as a function of gradient conditions.

---

#### **INTRODUCTION**

Reversed-phase gradient elution is today widely used for the separation and recovery of various purified products on a laboratory, pilot-plant and production scale. This is especially true for the case of large biomolecules: peptides and proteins, oligonucleotides and nucleic acids, and related compounds. The separation of these typically complex samples is affected by a large number of experimental variables whose role is often poorly understood. Recent studies [1–6] based on the computer modeling of reversed-phase gradient elution under preparative conditions have removed some of this uncertainty and we now possess the conceptual tools needed for a systematic examination of these separations.

---

<sup>a</sup> Present address: ProChrom, Indianapolis, IN 46278, U.S.A.

Other work [7-9] has shown that gradient elution runs are equivalent in most respects to "corresponding" isocratic separations (where a mobile phase %B is chosen to give similar retention as during gradient elution). In the present paper it will be shown that this analogy extends to the case of heavily-overloaded separations carried out in either an isocratic or gradient mode. This allows several conclusions previously reported for heavily overloaded isocratic elution [10] to be extended to corresponding gradient separations.

The present study makes use of computer simulations in order to show how the production rate ( $P_R$ , g/h) of purified product depends on various experimental conditions. Our aim will be to define general conditions that maximize  $P_R$  for a given sample. It should be noted that the present treatment is based on an idealized model (the Langmuir isotherm) that is known to be inapplicable in some respects for the high-performance liquid chromatographic separation of macromolecular (and other) samples. As a result, our goal in these studies is to develop some practical guidelines for preparative separations, not to attempt quantitative predictability for every case.

## THEORY AND BACKGROUND

### *Computer modeling*

The computer program (CRAIG4) used in the present study has been described [3,10,11]; it is based on a Craig distribution process and the Langmuir isotherm as an approximation to actual high-performance liquid chromatography (HPLC) systems. CRAIG4 allows the simulation of isocratic, gradient and step-gradient separations as a function of sample retention ( $k'$  values for a small sample), the column plate number, gradient conditions and sample size. In the present study, the samples are mixtures of two components X (first-eluted) and Y (the product). Various checks on the performance of CRAIG4 suggest that it is sufficiently reliable for the present application. The sample size ( $w/w_s$ ) which is entered into CRAIG4 must be 1.8 times larger than a corresponding experimental sample [10]. All sample sizes reported here have been so corrected, so as to correspond to experimental values, as in ref. 10. See the Symbols list at the end of this paper for the meaning of the standard symbols used here.

Similarly, column plate numbers  $N_0$  (small sample) are equal to  $[(\bar{k} + 1)/\bar{k}] n_c$ ;  $\bar{k}$  refers to the average  $k'$ -value during gradient elution of a small sample of the solute (see eqns. 1 and 2 below), and  $n_c$  is the number of Craig stages in a simulated run. The value of  $n_c$  was held constant during each Craig simulation.

### *Gradient vs. isocratic separation*

Previous work has established an overall similarity between isocratic and gradient separations for injection of either a small [7,8] or a large [9] sample, when "corresponding" conditions are used in both isocratic and gradient runs (reversed-phase HPLC). "Corresponding" conditions imply two requirements. First, all experimental parameters (column, flow-rate, etc.) have the same values in both runs, except that the mobile phase composition  $\phi$  is constant in the isocratic run and varies in the gradient run. Second, gradient steepness  $b$  is related to the capacity factor  $k'$  in the corresponding isocratic separation as

$$b = 1/1.15 k' \quad (1)$$

where

$$b = V_m \Delta\phi S / t_G F \quad (2)$$

Here,  $V_m$  is the column dead volume,  $\Delta\phi$  is the change in the volume fraction  $\phi$  of the B solvent during the gradient,  $t_G$  is the gradient time and  $F$  is the flow-rate. The solute-dependent parameter  $S$  is equal to the slope of a plot of isocratic values of  $k'$  vs.  $\phi$ . For "corresponding" conditions, such that eqns. 1 and 2 apply for each band (solute) in both the isocratic and gradient separation, it is found that sample resolution is the same in both cases (for both small and large samples).

#### *Maximum production rate $P_R$ for isocratic separation*

Previous work [10,12,14] has established certain relationships which define optimum conditions for preparative HPLC in an isocratic mode. The most important variable is the separation factor  $\alpha$ ; the mobile phase composition and column should usually be selected to provide a maximum value of  $\alpha$  for the product band Y and adjacent impurity bands X and Z on each side of band Y. The average value of  $k'$  for bands X and Y ( $k_x$  and  $k_y$ , small sample) has only a minor effect on production rate, as long as  $0.5 < k_x < 3$ .

Given values of  $k_x$  and  $\alpha$  for the separation, a decision is next required on the desired recovery (percentage of injected Y) of pure product from a single separation. Here (as previously) we define "pure" product as 99% Y plus 1% X, unless noted otherwise. The production rate  $P_R$  is strongly dependent [10] on the percentage recovery selected; e.g., relative  $P_R$  values of 1:3:10 for recoveries of 99.8%:95%:50%. Here a 95%-recovery will be assumed unless noted otherwise.

Once  $\alpha$ ,  $k_x$  and the percentage-recovery value have been defined, there is an optimum plate number  $N_o$  (small sample value) and sample size ( $w_y/w_s$ ), the weight of injected Y divided by the column capacity  $w_s$ ) for a maximum value of  $P_R$ . These relationships for isocratic separation are shown graphically in Fig. 1 (from ref. 12), for  $k_x = 1$ . Production rate  $P_R$  increases for larger  $\alpha$ :  $P_R \approx (\text{constant}) \cdot (\alpha - 1)^3$ .

As derived in the related study of production rate in isocratic separation [10], run time and the (small sample) plate number  $N_o$  (flow-rate and column length varied, pressure and other conditions constant) are related approximately as

$$\text{run time} = (\text{constant}) N_o^{4/3} \quad (3)$$

Production rate is given as

$$P_R = \frac{(\text{constant})(\text{weight of recovered product})}{(\text{run time})} \quad (4)$$

An arbitrary value of the constant in eqn. 4 is assumed; see ref. 10 for details. Run time is defined as the retention time  $t_g$  for the last-eluted band.

#### *Samples in which $S$ is not equal*

The value of the solute parameter  $S$  is determined mainly by solute molecular weight, and secondarily by other structural characteristics of the solute molecule.

## Optimum Sample size

## Optimum Plate Number

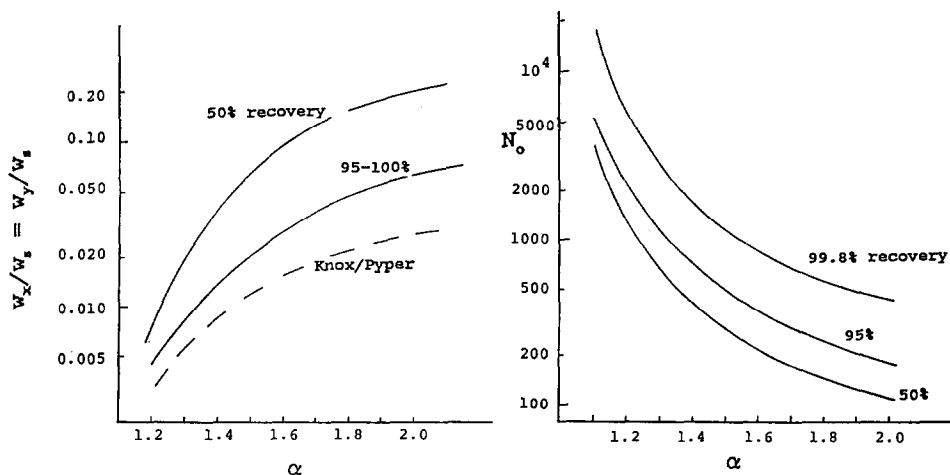


Fig. 1. Dependence of optimum sample size and plate number on  $\alpha$ , for maximum production rate (assumes  $k_x = 1$ , equal amounts of compounds X and Y in sample, specified recovery of Y). Taken from ref. 12.

Therefore, a product compound Y and its related impurity X will often have similar values of  $S$ . For this case (equal  $S$  values for X and Y), we will show in the present paper that production rate in gradient elution is governed by essentially the same relationships (Fig. 1 and related discussion) as for isocratic elution.

It is possible, however, for two compounds X and Y to have different values of  $S$ —even when X and Y are molecules of quite similar size and structure. This is particularly true for peptides and proteins, the  $S$  values of which appear to be strongly dependent on molecular folding and conformation. For example, the 14 000-dalton protein interleukin-2 can exhibit differences in  $S$  by a factor of as much as 3, as a result of the reduction of a single disulfide bond within the protein molecule plus substitution of a single amino acid by a different amino acid [14].

The preparative, gradient-elution separation of compounds X and Y having different values of  $S$  ( $S_x$  and  $S_y$ ) is very much affected by the ratio  $S_x/S_y$ . When  $S_x/S_y < 1$ , larger amounts of sample can be injected (other conditions the same) so that  $P_R$  is thereby increased. When  $S_x/S_y > 1$ , the opposite is true. This is schematically illustrated by the diagrams of Fig. 2, which relate isocratic retention as a function of  $\phi$  (straight-line plots) to corresponding gradient separations of a small and large sample (chromatograms).

When  $S_x = S_y$ , the plots of  $\log k'$  vs.  $\phi$  in Fig. 2A are parallel, and the separation factor  $\alpha$  is constant as  $\phi$  is varied. As sample size increases in gradient elution, the sample bands X and Y are eluted in a progressively weaker mobile phase (smaller values of  $\phi$ ), but  $\alpha$  remains constant. When  $S_x < S_y$  (Fig. 2B),  $\alpha$  is seen to increase for smaller  $\phi$ , and also for a larger sample in gradient elution. The result is a better separation of the sample. When  $S_x > S_y$  (Fig. 2C),  $\alpha$  decreases as the sample size

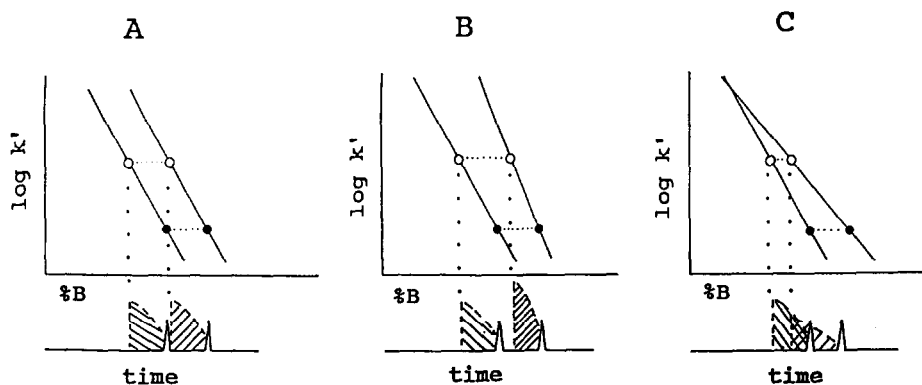


Fig. 2. Relation of isocratic retention ( $k'$ ) as a function of mobile-phase composition (%B) to maximum sample size in preparative separation by gradient elution. See text and ref. 5 for details.

increases, with a resulting poorer separation. For the further discussion of Fig. 2, see ref. 5.

When solute  $S$  values differ appreciably (by  $> 2\%$ ), the corresponding conditions for maximum production rate in preparative gradient elution may also differ. This situation is examined further in the present study.

## RESULTS AND DISCUSSION

### *Experimental conditions for maximum production rate $P_R(S_x = S_y)$*

*Optimum values of sample size and column plate number.* The approach followed in ref. 10 and in the present study is illustrated in Figs. 3 and 4 for a fixed set of gradient conditions:  $\bar{k} = (1/1.15b) = 0.87$ ,  $\alpha = 1.7$ ; the starting value of  $k_o$  (defined as  $k_{og}$ ) = 10 for solute X and 17 for solute Y ( $k_o$  refers to  $k'$  for a small sample). Fig. 3 shows the

$w_y/w_x =$	0.04	0.05	0.06	0.07
	99/99	98/97	92/96	82/92

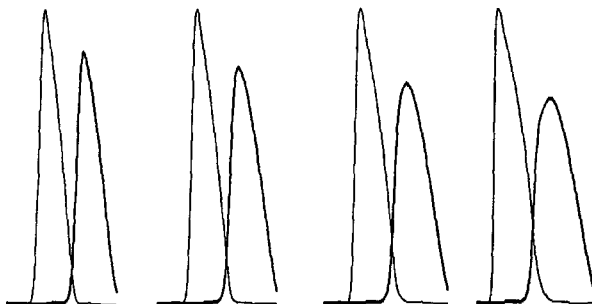


Fig. 3. Computer simulations (CRAIG4) of preparative separation by gradient elution as a function of sample size. Conditions:  $k_{og} = 10$  and 17 for X and Y ( $\alpha = 1.7$ );  $N_o = 400$ ;  $b = 1.00$  ( $k = 1$ ); equal amounts of X and Y in sample.

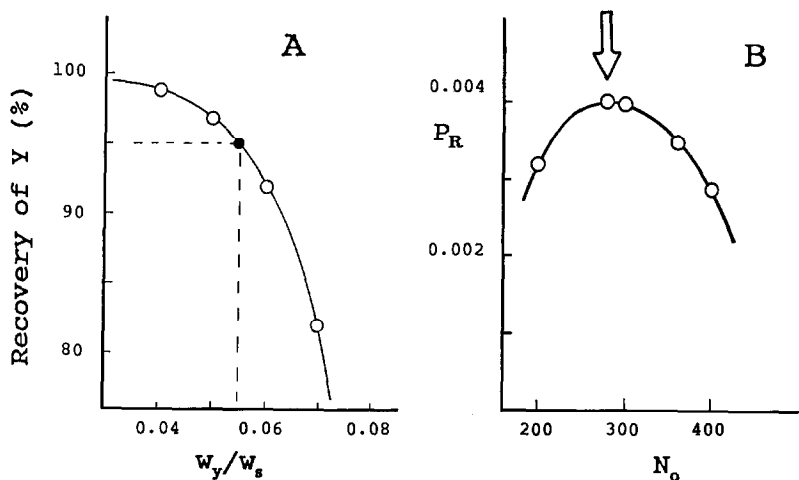


Fig. 4. Determination of conditions for maximum production rate in preparative gradient elution. (A) Determination of sample size for 95% recovery of 99%-pure Y; conditions of Fig. 3. (B) Plot of production rate (for 95% recovery of Y) vs. column plate number; procedure of Figs. 3 and 4A repeated for other plate numbers as indicated.

resulting separations for different sample sizes and a plate number  $N_o = 400$ . It is assumed here and elsewhere that the weights of X ( $w_x$ ) and Y ( $w_y$ ) in the sample are equal; later in this paper we will examine the case of unequal values of  $w_x$  and  $w_y$ . The numbers (e.g., 92/96 for  $w_y/w_s = 0.06$ ) in Fig. 3 refer to the recoveries of 99%-pure X (92%) and Y (96%) respectively.

In Fig. 4A the recoveries of pure Y (from Fig. 3) are plotted vs. sample size. We can select optimum conditions for any desired recovery of pure product; in the present study we will assume that 95% recovery is desired. By analogy with the study of ref. 11 for isocratic separation, it can be assumed that maximum production rate will be 3-fold less on average for a 99.8% recovery of pure Y, and 3-fold greater for a 50% recovery of pure Y. In Fig. 4A it is seen that 95% recovery of Y corresponds to a sample size of  $w_y/w_s = 0.055$ ; i.e., 5.5% of the column saturation capacity.

The procedure of Figs. 3 and 4A was next repeated for other values of the column plate number  $N_o$ , yielding values of sample size (for 95% recovery) as a function of  $N_o$ . Eqns. 3 and 4 were then used to obtain values of  $P_R$  vs.  $N_o$ , and these are plotted in Fig. 4B. It is seen that a maximum production rate can be obtained with a plate number of about 280. That is, for these gradient conditions ( $\alpha = 1.7$ ,  $b = 1.00$ , and  $k_{og} = 10$  for X) we have established the sample size ( $w_y/w_s = 0.04$ ) and plate number ( $N_o = 280$ ) that yields a maximum production rate ( $P_R = 0.004$ ; arbitrary units, see ref. 10). As observed previously [10] for isocratic separation, production rate is not greatly affected if somewhat different values of  $N_o$  are used; e.g.,  $200 < N_o < 400$ .

*Sample size vs. plate number.* As the plate number  $N_o$  is increased, it is possible to inject a larger sample for the same (95%) recovery of pure product (Y). This is shown in Fig. 5A, where the amount of Y that can be injected (95% recovery of 99%-pure Y) is plotted vs.  $N_o$ . The plate number for maximum production rate (optimum  $N_o$ ) is shown as a dark point on each curve. For each value of  $\alpha$  there is a minimum plate

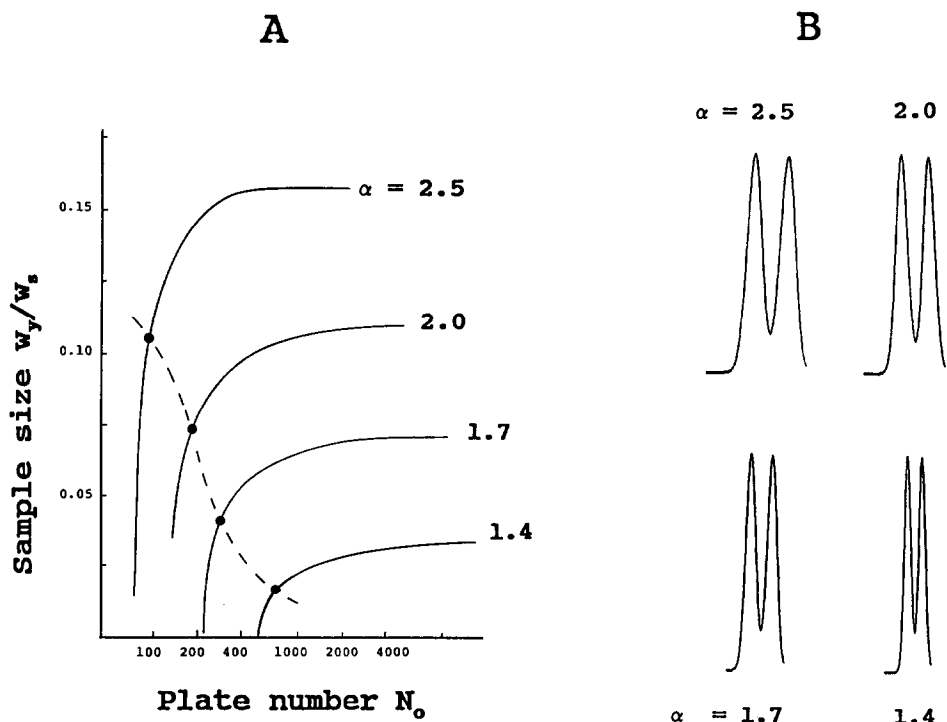


Fig. 5. Comparisons (as in Fig. 4B) of maximum sample size for 95% recovery of 99%-pure product as a function of plate number  $N_o$  and  $\alpha$ . Conditions:  $k_{og}$  for  $X = 10$ ,  $b = 1.00$ . (A) All data;  $\bullet$  = conditions for maximum production rate for a given value of  $\alpha$ . (B) Chromatograms for separations of (A) that correspond to maximum production rate [designated by  $\bullet$  in (A)].

number required, below which the desired recovery (95%  $Y$ ) is not possible. Likewise, the maximum sample size levels off to a constant value for plate numbers somewhat larger than the optimum value of  $N_o$ . This is strongly reminiscent of the findings of Knox and Pyper [12] for isocratic touching-band separations. It should also be noted that the optimum sample size (for an optimum value of  $N_o$ ) in isocratic touching-band separations is about 2/3 of the maximum sample size for a large value of  $N_o$  (eqn. 16a of ref. 13, with  $q = 3$ ); the corresponding optimum sample size in Fig. 5B is 50–65% as large as the maximum sample size for large  $N_o$  (i.e., similar to the value of 67% for touching-band separations [12]).

For isocratic separations with 95% recovery of pure product, it was observed [10] that a small-sample separation with the optimum plate number gives a resolution of the two bands ( $X$  and  $Y$ ) of  $R_s = 1.18 \pm 0.06$ ; i.e., a constant value that can be used to verify that an optimum value of  $N_o$  has been selected for a given separation. Fig. 5B shows the corresponding small-sample separations that correspond to the optimum values ( $\bullet$ ) of Fig. 5A. The resolution of these various separations is again constant, with  $R_s = 1.1$ – $1.2$ . This is essentially the same result found for isocratic separation; i.e., the similarity of isocratic and gradient elution is again confirmed.

*Effect of initial mobile phase composition.* The choice of initial mobile phase

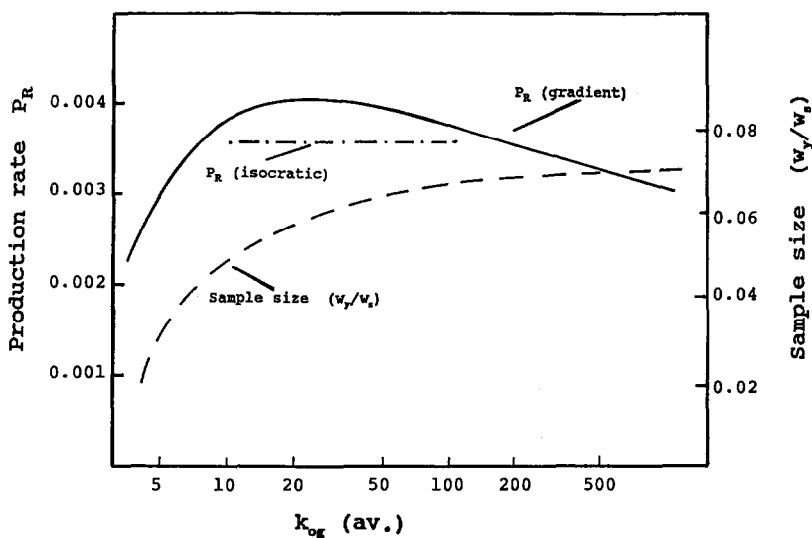


Fig. 6. Production rate (for 95% recovery of Y) in preparative gradient elution as a function of the starting mobile phase (which determines  $k_{og}$  for X and Y). Conditions: (gradient runs)  $\alpha = 1.7$ ,  $N_o = 280$ ,  $b = 1.0$ , sample size adjusted to yield 95% recovery of 99%-pure Y; (isocratic runs)  $\alpha = 1.7$ ,  $N_o = 300$ ,  $k_x = 1.0$ , sample size adjusted for 95% recovery of Y. Equal amounts of X and Y in sample.

composition ( $\varphi$  or %B) determines the values of  $k'$  ( $k_{og}$ ) at the beginning of separation; the larger  $\varphi_o$ , the smaller is  $k_{og}$ . This will in turn affect: (a) the amount of sample that can be injected (for 95% recovery of 99%-pure product) and (b) the resulting production rate.

Computer simulations were carried out for different values of  $k_{og}$  ( $k_{og} = 10$  and 17 for X and Y, respectively, in the example of Figs. 3 and 4), in order to determine production rate as a function of  $k_{og}$ . These are summarized in Fig. 6 for the same conditions as above ( $\alpha = 1.7$ ,  $b = 1.00^a$ ), except that the initial mobile phase is allowed to change so as to vary the  $k_{og}$  values of solutes X and Y. Values of the optimum sample size  $w_y/w_s$  (95% recovery of Y) were determined first for each value of  $k_{og}$ , in the same manner as in Figs. 4 and 5A. These values are plotted in Fig. 6 (dashed curve) and are seen to increase with larger values of  $k_{og}$  (av.). The run time increases also with  $k_{og}$ , so that production rate (eqn. 4) passes through a maximum value for  $k_{og} (av.) \approx 25$ . This is a quite flat maximum, however, so that production rate is roughly the same for  $8 < k_{og} < 100$ ; i.e., the choice of the initial mobile phase composition can be varied somewhat without affecting production rate.

Also noted in Fig. 6 is the production rate for the corresponding isocratic separation (— · —); i.e., for  $k_x = 1$ ,  $k_y = 1.7$ , and  $\alpha = 1.7$ . The maximum production rates for the corresponding isocratic and gradient separations (for an optimum value of  $k_{og}$ ) are seen to be similar ( $P_R = 0.0036$  vs. 0.0042).

<sup>a</sup> The optimum plate number  $N_o = 280$  determined in Fig. 4B was held constant in these computer simulations. Reoptimizing  $N_o$  for each value of  $k_{og}$  did not change the maximum value of  $P_R$  by more than 5–10% (see later discussion of Fig. 12).



TABLE I

PRODUCTION RATE  $P_R$  AS A FUNCTION OF SEPARATION CONDITIONS FOR EITHER ISOCRATIC OR GRADIENT ELUTION

Conditions ( $k_{og}$ ,  $w_x = w_y$ ,  $N_o$ ) selected for maximum  $P_R$ ;  $b = 1.00$ ,  $S_x = S_y$ .

$\alpha$	Optimum	$N_o$		$w_y/w_x$		$P_R$	
		Isocratic	Gradient	Isocratic	Gradient	Isocratic	Gradient
1.40	6-100	700	700	0.014	0.018	0.0004	0.0005
1.70	8-100	300	280	0.03	0.04	0.004	0.004
2.00	8-150	180	180	0.07	0.08	0.02	0.02
3.00	25-200	80	60	0.16	0.14	0.04	0.08

*Effect of the separation factor  $\alpha$ .* The simulations summarized in Fig. 6 for  $\alpha = 1.7$  were repeated for other values of  $\alpha$ , with the results of Table I. It is seen that the optimum values of the plate number  $N_o$  and sample size ( $w_x/w_s$ ) are generally similar for both isocratic and gradient elution, as are values of the maximum production rate for a given value of  $\alpha$ . This is further illustrated in Fig. 7 where maximum values of  $P_R$  are plotted vs.  $\alpha$  for both isocratic (— — —) and gradient (—) elution.

The lower production rate for isocratic vs. gradient elution (Fig. 7) at high values of  $\alpha$  is mainly an artifact of Craig simulation. Thus the isocratic Craig plate number  $N_o$  is lower for the second band relative to the first (for a fixed value of  $n_c$ ,  $N_o$  decreases

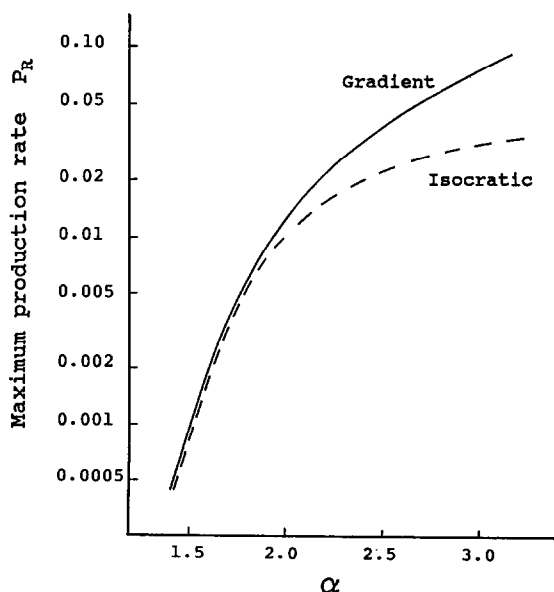


Fig. 7. Maximum production rate (95% recovery of Y, optimized values of  $N_o$  and  $w_y/w_s$ ) for isocratic and gradient elution as a function of  $\alpha$ . Data of Table I.

with increasing  $k'$ ), and this difference becomes larger for larger values of  $\alpha$ . In gradient elution, on the other hand, the plate numbers for both bands are equal (because values of  $\bar{k}$  are equal). Since the value of  $N_o$  reported in Table I for isocratic separations is for the first band X, the average  $N_o$ -value for the two bands (not used in calculating  $P_R$ ) is therefore smaller for isocratic separation vs. gradient elution. This has the effect of (artificially) lowering production rate for isocratic vs. gradient elution.

*Effect of gradient steepness  $b$ .* By analogy with isocratic separation [10] we would expect maximum production rate in gradient elution to be relatively insensitive to gradient steepness, as long as  $0.5 < \bar{k} < 3$  (or  $0.3 < b < 2$ ). Craig simulations of preparative gradient elution were carried out to confirm this prediction; some representative data ( $\alpha = 1.7$ ,  $k_{og}$  for X = 10) are shown in Fig. 8A ("gradient" curve) as a function of  $\bar{k}$ . Corresponding data for isocratic separation ("isocratic" curve) are plotted in Fig. 8 vs.  $k'$  ( $k_o$ ) for compound X. It is seen that a maximum production rate in gradient elution is favored by somewhat higher values of  $\bar{k}$  ( $2 < \bar{k} < 5$ ) vs. optimum values of  $k'$  in isocratic elution ( $0.5 < k' < 3$ ). Part of this difference arises from the fact that  $\bar{k}$  is equal for both X and Y, whereas  $k'$  for Y is 1.7-fold greater than for X. The difference between optimum values of  $k'$  or  $\bar{k}$  in isocratic and gradient elution therefore becomes smaller for smaller values of  $\alpha$  ( $\alpha = 1.7$  in Fig. 8).

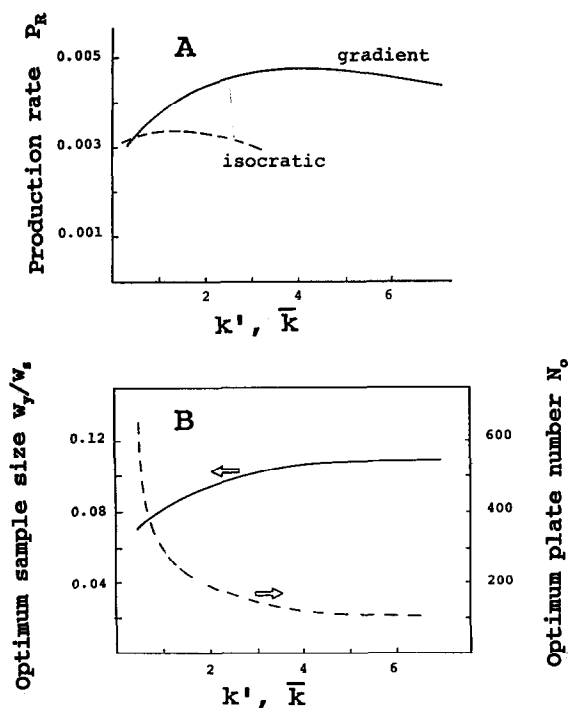


Fig. 8. Effect of average sample retention ( $k'$  or  $k$ ) on production rate and sample size in isocratic and gradient elution. (A) Maximum production rate (95% recovery of Y) as a function of gradient steepness ( $\bar{k}$ ) or isocratic solvent strength ( $k'$ ). Conditions: (gradient)  $k_{og}$  for X = 10,  $N_o$  and  $w_y/w_x$  optimized for maximum  $P_R$ ; (isocratic)  $N_o$  and  $w_y/w_x$  optimized for maximum  $P_R$ ; equal amounts of X and Y in sample. (B) Optimum sample size and plate number (both isocratic and gradient; same values) as a function of sample retention. Conditions as in Fig. 6 unless noted otherwise.

Fig. 8B shows how optimum values of sample size and plate number vary with the choice of  $\bar{k}$  or  $k'$ . There is little difference in the optimum values shown here for isocratic vs. gradient elution. This represents another example of the close similarity of preparative separations for corresponding isocratic and gradient elution systems.

*Experimental conditions for maximum production rate  $P_R(S_x \neq S_y)$*

The preparative gradient-elution separation of samples where  $S_x \neq S_y$  has been examined briefly in ref. 5. CRAIG4 simulations used in that study demonstrated that higher sample loads are possible when  $S_x < S_y$  and vice versa for  $S_x > S_y$ , as can be inferred from Fig. 2 in this paper. Thus larger samples elute earlier (in a mobile phase of lower %B), which means smaller average values of  $\alpha$  for the case where  $S_x > S_y$  (Fig. 2C) and *vice versa* for  $S_x < S_y$ .

If the gradient steepness  $b$  is decreased, small-sample resolution will increase for the case of  $S_x = S_y$ , because  $\bar{k}$  increases (and  $\alpha$  remains constant) as  $b$  becomes smaller. A similar beneficial effect of flatter gradients is observed in preparative separations, in that better separations result—which means that larger samples can be separated for some required purity and recovery of the product. If  $S_x \neq S_y$ , a change in  $b$  should have a somewhat different effect on sample separation. Thus a flatter gradient means a larger value of  $\bar{k}$ , and elution of the sample in a mobile phase of smaller %B. From Fig. 2 it can be inferred that resolution will then increase more slowly with decrease in gradient steepness  $b$  when  $S_x > S_y$ , and more rapidly when  $S_x < S_y$ . The same should also be true of preparative separations, which means that the optimum value of  $b$  will be lower (vs. the value of  $b \approx 0.2$  suggested by Fig. 8A for the case of  $S_x = S_y$ ) when  $S_x > S_y$ , and higher when  $S_x < S_y$ .

Similar logic suggests that optimum values of  $k_{og}$  should be larger for the case of  $S_x > S_y$ , and smaller when  $S_x < S_y$ .

*Effect of sample size.* Fig. 9 summarizes a number of CRAIG4 simulations for the same gradient conditions as in Fig. 3 and 4 ( $N_o = 280$ , average value of  $k_{og}$  equal  $[(10 + 17)]/2 = 13.5$ ,  $\alpha = 1.7$ ,  $b = 1$ ) but with different ratios of  $S_x/S_y$  (corresponding to different samples) and different sample sizes. Values of  $k_{og}$  were selected to give the same resolution ( $R_s = 1.1$ ) for a small sample ( $w_y/w_s = 10^{-3}$ ). Thus for an average value of  $k_{og} = 13.5$ , individual values of  $k_{og}$  for bands X and Y were 9.3 and 17.8 for  $S_x/S_y = 1.05$ , compared to  $k_{og} = 10$  (X) and 17 (Y) for  $S_x/S_y = 1.05$ . The resolution of X and Y for a small sample was in each case intentionally the same, in order to compare the contrasting effects of increasing sample size for separations where  $S_x/S_y$  is different.

As sample size is increased, the separation for the sample with  $S_x/S_y = 1.1$  (unfavorable case) is seen to quickly overload, and for the last chromatogram ( $w_y/w_s = 0.09$ ) the recovery of 99%-pure Y is only 28%. For the sample with  $S_x/S_y = 1.0$  ("normal" case), there is less band overlap as the sample size is increased. For a sample size of  $w_y/w_s = 0.09$ , the recovery of 99%-pure Y is 68%; *i.e.*, much greater than for the sample with  $S_x/S_y = 1.1$ .

For the bottom sample of Fig. 9 ( $S_x/S_y = 0.9$ ; favorable case), there is little band overlap for any of these sample sizes. The recovery of 99%-pure Y is about the same (99%) regardless of sample size, and a much larger sample could be injected with 95%+ recovery of Y. These examples emphasize the importance of the relative values of  $S$  for compounds X and Y; the production rate increases (other factors equal) as  $S_y/S_x$  increases.

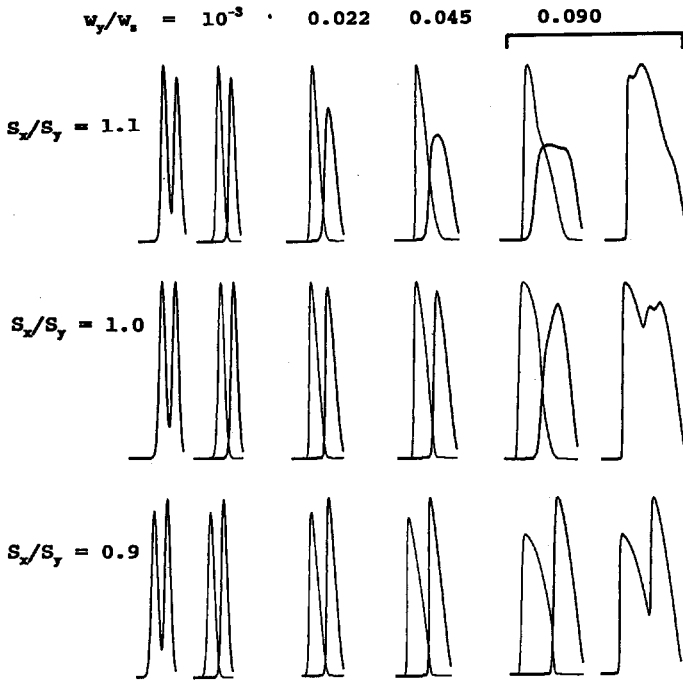


Fig. 9. CRAIG4 simulations for separation as a function of the sample (different values of  $S_x/S_y$ ) and sample size ( $w_x = w_y$ ). Conditions:  $k_{0g}$  (av.) = 13.5,  $b = 1$ ;  $\alpha = 1.7$  for  $S_x = S_y$ ;  $k_{0g}$  values for other samples ( $S_x \neq S_y$ ) selected to give equal  $R_s$  for a small sample;  $N_0 = 280$ .

*Optimum values of the gradient steepness  $b$ .* The effect of a change in gradient steepness on both small-sample and preparative separations is illustrated by the computer simulations of Fig. 10. For purposes of comparison, we have chosen sample conditions (values of  $k_{0g}$ ) such that the same small-sample resolution ( $R_s = 1.05$ ) is obtained for  $b = 1$  (the value of  $R_s$  for each small-sample separation in Fig. 10 is indicated over the two bands). The large-sample recoveries of X and Y (shown in Fig. 10) are seen to be greater (94% of X, 89% of Y) for  $b = 1$  and  $S_x = 9.5$ ,  $S_y = 10.5$ , vs. the case of larger ratios of  $S_x/S_y$ ; e.g., 37% recovery of X and 35% of Y for  $S_x/S_y = 10.5/9.5$ . This is the same effect of sample size seen in Fig. 9.

Looking first at the small-sample separations, we see in Fig. 10 that resolution increases for all three samples (top, middle and bottom) as  $b$  decreases. However, resolution increases with  $b$  faster for the sample with  $S_x/S_y = 9.5/10.5$  and slower for the sample with  $S_x/S_y = 10.5/9.5$ . That is, small-sample resolution is relatively better for the former sample at lower values of  $b$ , and vice versa for the latter sample — as predicted by our discussion of Fig. 2.

In similar fashion, we see in Fig. 10 (large-sample separations) that the recovery of pure product increases with decrease in  $b$  much faster for the top separations ( $S_x = 9.5$ ,  $S_y = 10.5$ ) vs. the bottom separations ( $S_x = 10.5$ ,  $S_y = 9.5$ ) — again as predicted by theory. Specifically, the recovery of Y in the bottom separations increases hardly at all as  $b$  decreases, which means that the production rate *decreases* as

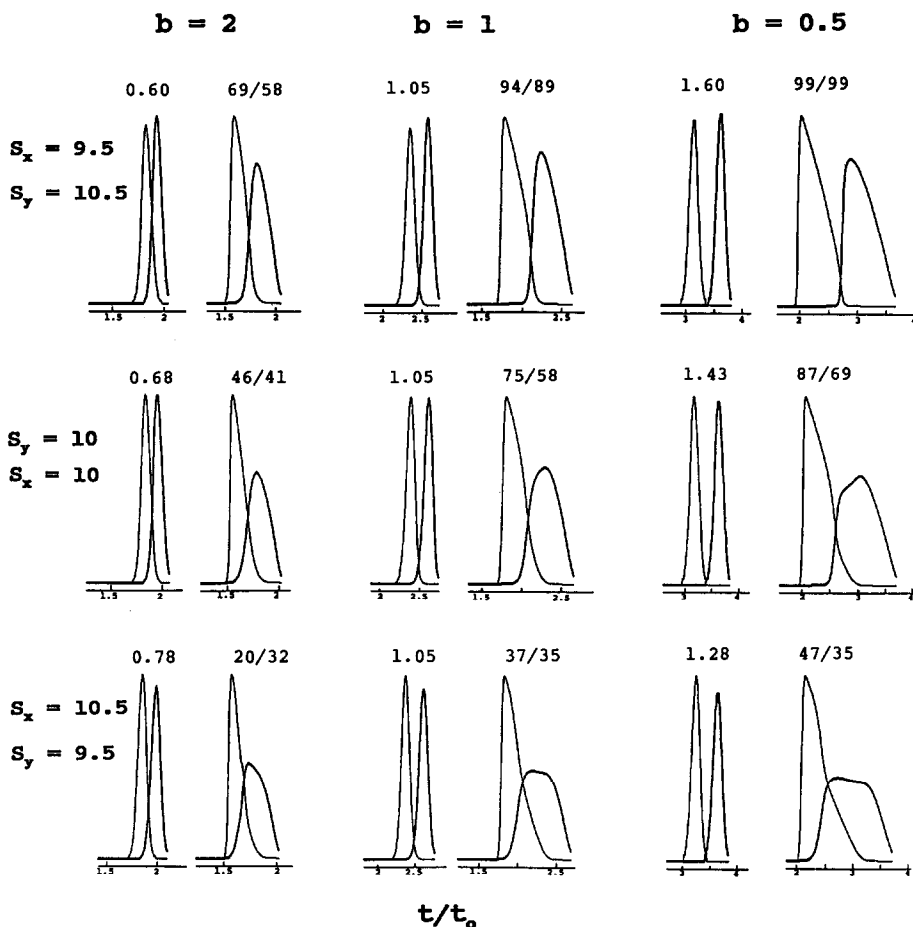


Fig. 10. CRAIG4 simulations for separation as a function of the sample (different values of  $S_x/S_y$ ) and gradient steepness  $b$ . Two sample sizes are shown for each set of conditions:  $w_x = w_y$  with  $w_x/w_y = 0.001$  and  $0.09$ , respectively; sample resolution  $R_s$  is indicated for the first (small-sample) separation, and values of percentage recovery of 99%-pure product (X/Y) are indicated for the second (large-sample) separation. Conditions:  $k_{og}(\text{av.}) = 13.5$ ;  $\alpha = 1.7$  for  $S_x = S_y$ ;  $k_{og}$  values for other samples ( $S_x \neq S_y$ ) selected to give equal  $R_s$  for a small sample and  $b = 1$ .  $N_o = 280$  ( $n_c = 91, 140$  and  $191$  for  $b = 2, 1$  and  $0.5$ , respectively).

$b$  decreases (because run time increases as  $b$  decreases). This is in contrast to an optimum value of  $b \approx 0.2$  for the middle case ( $S_x = S_y$ , see Fig. 8A). It can therefore be concluded that the optimum value of  $b$  is  $> 0.2$  when  $S_x > S_y$ , and  $< 0.2$  when  $S_x < S_y$ .

*Optimum values of  $k_{og}$ .* Fig. 11 presents computer simulations similar to those of Fig. 10, but with gradient steepness held constant while the initial mobile-phase composition is varied so as to vary values of  $k_{og}$ . The reference separations (with a small-sample resolution of  $R_s = 1.05$  for each sample) are for  $k_{og}(\text{av.}) = 13.5$  (first column of chromatograms). As the initial value of %B is decreased (so that  $k_{og}$  values

$k_{og} \text{ (av.)} = 13.5$ 

135

1350

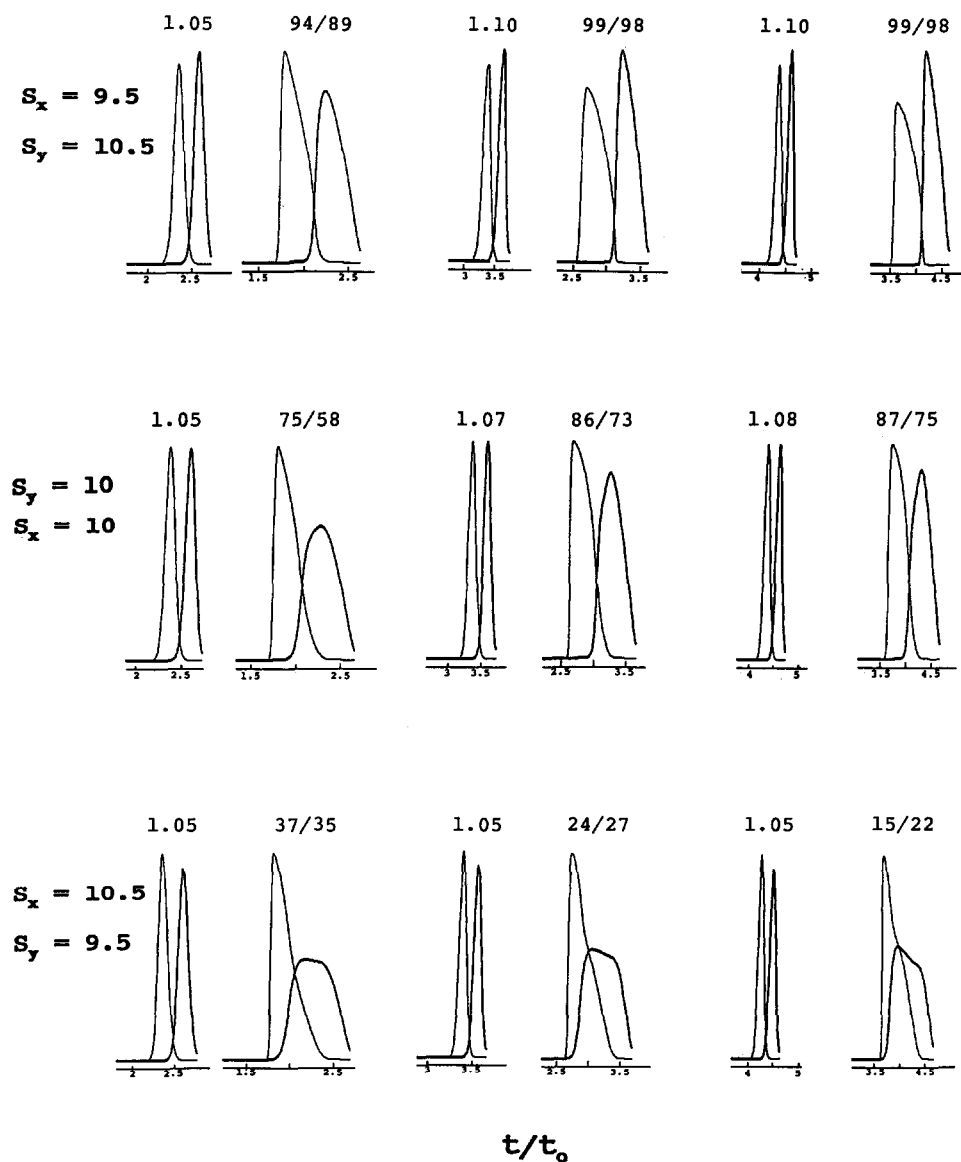


Fig. 11. CRAIG4 simulations for separation as a function of the sample (different values of  $S_x/S_y$ ) and initial mobile-phase composition (values of  $k_{og}$ ). Two sample sizes are shown for each set of conditions:  $w_x = w_y$  with  $w_x/w_y = 0.001$  and  $0.09$ , respectively; sample resolution  $R_s$  is indicated for the first (small-sample) separation, and values of percentage recovery of 99%-pure product (X/Y) are indicated for the second (large-sample) separation. Conditions:  $b = 1.00$ ;  $\alpha = 1.7$  for  $S_x = S_y$ ;  $k_{og}$  values for other samples ( $S_x \neq S_y$ ) selected to give equal  $R_s$  for a small sample and  $k_{og} \text{ (av.)} = 13.5$ .  $N_0 = 280$  ( $n_c = 140$ ).

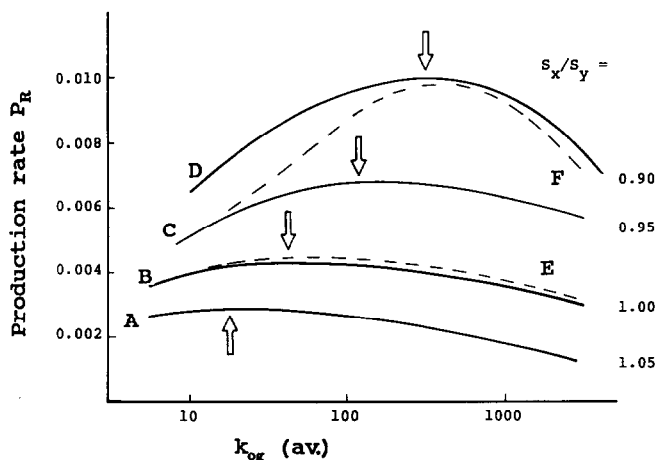


Fig. 12. Production rate (95% recovery of Y) as a function of initial mobile-phase composition (av. value of  $k_{og}$  for X and Y). Conditions:  $\alpha = 1.7$ , av.  $\bar{k} = 1.00$  ( $b = 0.87$ ); (A–D)  $N_o = 280$ ; (E–F)  $N_o$  optimized for maximum production rate. Equal amounts of X and Y in sample. See text for further details.

increase)<sup>a</sup>, it is seen that there is a modest increase in  $R_s$  for the small-sample separations when  $S_x < S_y$ , but no change in  $R_s$  for the sample with  $S_x > S_y$ . That is, a larger value of  $k_{og}$  generally favors small-sample resolution, except when  $S_x > S_y$ .

Similarly the recovery of pure product from the large-sample separations increases with increasing  $k_{og}$  when  $S_x < S_y$ , but the opposite is true for samples with  $S_x > S_y$ —as expected from Fig. 2. Data as in Fig. 11 can be generalized as before, in terms of plots of production rate  $P_R$  vs. average values of  $k_{og}$  for two bands X and Y (Fig. 12). The solid curves (A–D) of Fig. 12 correspond to separations where  $N_o$  is constant (equal to 280), and  $S_x/S_y$  varies; a difference in maximum production rate by a factor of four is seen as  $S_x/S_y$  varies from 1.05 to 0.90. Fig. 12 also shows that the optimum value of  $k_{og}$  (av.) increases for smaller values of  $S_x/S_y$ —as expected from the discussion of Fig. 2. That is, for  $S_x/S_y < 1$ ,  $\alpha$  increases as  $\varphi$  decreases and  $k_{og}$  (av.) increases; this favors a larger initial value of  $k_{og}$  (av.).

The dashed curves (E, F) of Fig. 12 are corresponding plots of  $P_R$  (for  $S_x/S_y = 1.00$  and 0.95, respectively) where  $N_o$  is allowed to vary so as to maximize production rate (as in Fig. 3B). In the case of equal values of  $S$  (curves B and E), there is little difference in the possible production rate as a function of  $k_{og}$  (av.). However, when  $S_x < S_y$  (curves C and F), the optimization of  $N_o$  (smaller values) leads to a further increase in  $P_R$  and to an optimum value of  $k_{og}$  (av.) which is larger.

Additional CRAIG4 simulations for other values of  $\alpha$  and  $k$  show the same trends as in Fig. 12 for  $\alpha = 1.7$  and  $k = 1$ . That is, production rate can be significantly

<sup>a</sup> The change in values of  $k_{og}$  with change in %B is assumed to be given by  $\log k' = \log k_w - S\varphi$ , which is generally a good approximation for reversed-phase separation. Here  $k_w$  is the value of  $k'$  for water as mobile phase. A similar relationship is observed for ion-exchange separations where the charge on the solute molecule is  $\geq 2$  (generally the case for proteins) and for separations by hydrophobic interaction chromatography [17].

higher for samples where  $S_x < S_y$ , and the gradient for such samples should start at a lower value of %B, vs. the case where  $S_x/S_y > 1$ .

*Purification vs. separation: the case where X or Y is a major component of the sample*

Quite often the objective of a preparative HPLC separation by gradient elution of a peptide or protein sample is the purification of a material that is already 90–99% pure. That is, the relatively higher cost of HPLC purification makes its use more

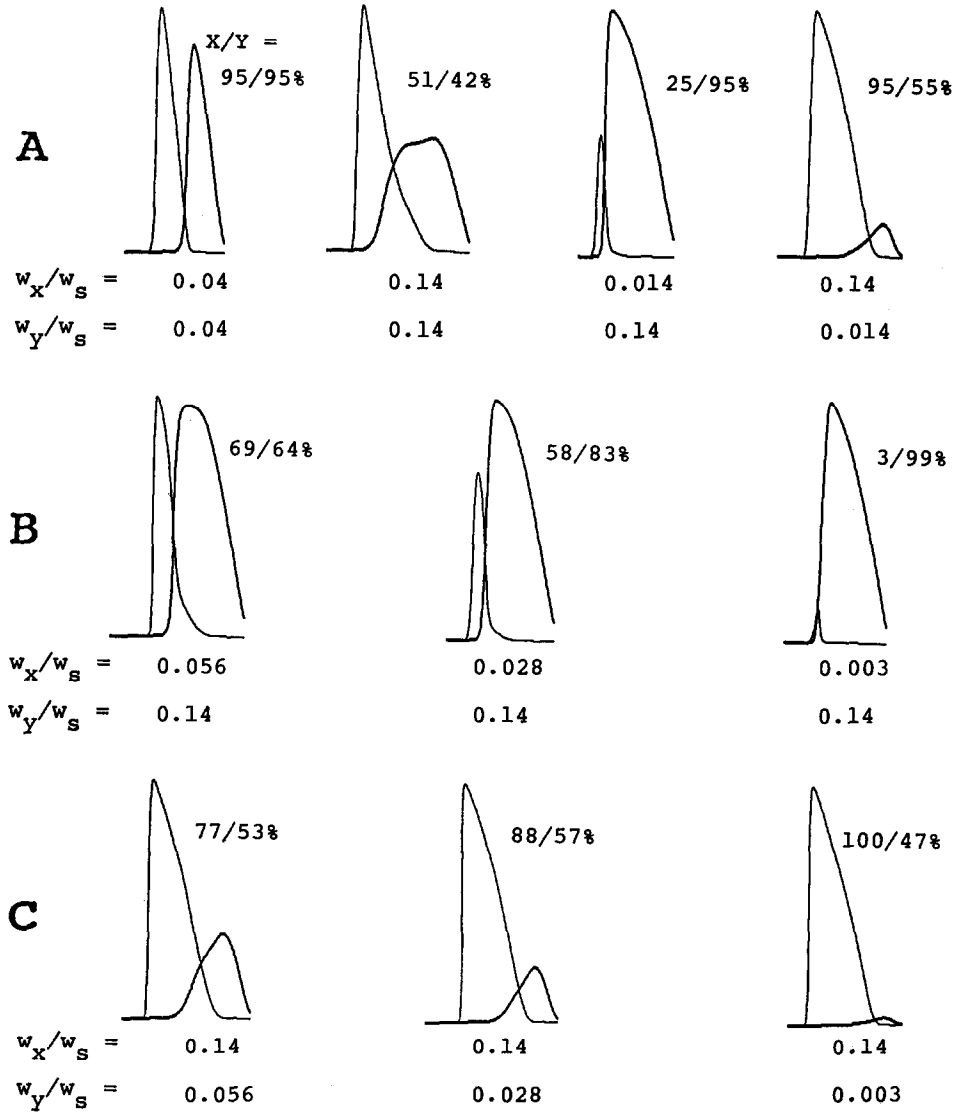


Fig. 13. CRAIG4 simulations for samples where relative concentrations of X and Y vary. Conditions:  $\alpha = 1.7$ ,  $k_{og}$  for X equal 10;  $k = 1$ ,  $N_o = 280$ . X/Y values are recoveries of 99%-pure X and Y, respectively.



attractive at the end of a separation/purification sequence—for a “final polish” of the product. The question then arises as to how our conclusions for the case of samples containing equal amounts of an impurity X and a product Y will be altered.

Previous (limited) studies of isocratic separation based on computer simulation [10] suggest that larger amounts of a more-pure product can be charged, *vs.* the case of less-pure feed material. For example, if the feed material is 90%-pure X or Y, rather than 50%-pure as in the preceding examples, it was found that about 4 times as much product could be injected (for 95% recovery of X or Y). This in turn increases production rate by 4-fold. The ability to inject larger amounts of purer product in preparative HPLC seems intuitively obvious, and this conclusion matches the experience of practical workers.

We have examined the role of feed purity in preparative gradient elution, using CRAIG4 simulations with similar conditions as in our earlier examples ( $\alpha = 1.7$ ,  $k_{og} = 10$  and 17 for X and Y,  $b = 1$ ). Some examples are shown in Fig. 13. In Fig. 13A, a sample size of  $w_x/w_s = w_y/w_s = 0.04$  gives 95% recovery of 99%-pure X or Y; *i.e.*, the reference case we have used so far for our calculations of production rate. For a sample 3.4-times as large ( $w_x/w_s = w_y/w_s = 0.14$ , second example in Fig. 13A), the band overlap is much more serious—as expected, and the recovery of pure X and Y (51 and 42%) drops sharply. For the same weight of either X or Y, but a 10-fold lower concentration of the other compound in the sample (last two examples in Fig. 13A), 95% recovery of pure X or Y (whichever is the major component) is possible. This is similar to the situation observed for isocratic separation [10], where a 4-fold (*vs.* 3.4-fold for gradient) larger weight of product could be injected for the same recovery of pure product—when the contamination of the feed is 10-fold less.

Figs. 13B and C show other simulations, for samples whose composition varies in terms of the relative concentrations of X and Y: 0.4/1 (B) or 1/0.4 (C) in the first example, 0.2/1 (B) and 1/0.2 (C) in the second example, and 0.02/1 (B) and 1/0.02 (C) in the last example. In each case, the weight of the major component is held constant at  $w/w_s = 0.14$ . The recovery of 99%-pure product (either X or Y) is again indicated as the value of X/Y (see example of Fig. 3).

It is also useful to examine the role of feed composition and separation from a different standpoint. That is, in some cases we wish to specify some minimum purity in the final product; *e.g.*, 99% as in the preceding examples. However, it is also useful to specify the relative removal of an impurity from the feed; *e.g.*, 90% removal, which for an initial impurity concentration of 10% would mean a final concentration in the purified product of 1%. If we plot the results of Fig. 13 in this way, for removal of either X or Y from the initial sample (feed) with 95% recovery of purified product, the graph of Fig. 14 results. The solid curve is for the removal of compound X as impurity, while the dashed curve shows the removal of compound Y. It is noteworthy in this example that for impurity (minor component) concentrations of less than 15% [corresponding to a (minor component/major component) ratio  $< 0.2$  in the feed], the relative removal of the impurity is about the same (88–91%, for 95% recovery of product), regardless of the impurity concentration in the feed. This suggests that the elution pattern of the impurity is largely determined by the weight of the product band—when the impurity is present in less than 15% relative concentration. This seems intuitively reasonable, and the various examples of Fig. 13 (excluding the first two chromatograms of Fig. 13A, where  $w_x = w_y$ ) provide visual confirmation of this observation.

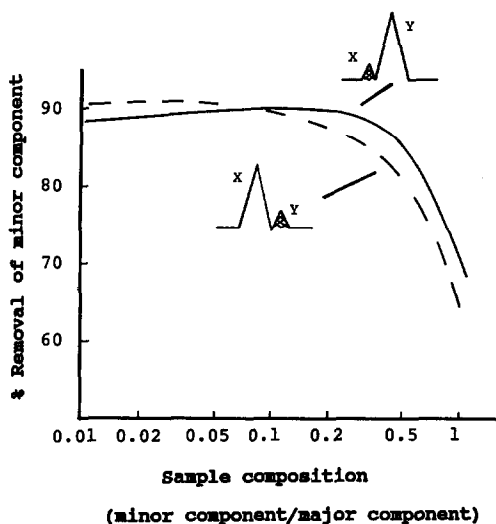


Fig. 14. Relative removal of sample impurity (minor component) as a function of sample composition (concentrations of X and Y), for 95% recovery product (major component). Conditions: constant weight of product in injected sample ( $w/w_s = 0.14$ );  $\alpha = 1.7$ ,  $k_{og}$  for X equal 10;  $b = 1$ ).

Now consider the case where it is desired to purify a feed that is initially  $> 80\%$  product. If the purification goal can be expressed as some fractional removal of the impurity(s), e.g., 90% as in Fig. 14, then the actual composition of the feed is immaterial. That is, the impurity concentration in the feed can vary from 0–20%, and the same percentage-removal of impurity (for some required recovery (e.g., 95%) of product will be obtained for a given set of separation conditions: same weight of product charged, same gradient conditions, etc. This generalization can considerably simplify the design of an optimum separation for the case where the feed composition varies from batch to batch.

## CONCLUSIONS

In the present study we have begun to define experimental conditions that maximize the production rate of purified product in heavily overloaded separations by gradient elution. It has been shown previously that there is a close similarity between isocratic and gradient elution for either: (a) the separation of small samples or (b) preparative separations where the product band just begins to overlap an adjacent impurity band ("touching-band" separation). Similar separations result in each case (isocratic or gradient elution) when "corresponding" conditions are used (such that  $k' = \bar{k}$ ). This similarity between isocratic and gradient elution is maintained for separations involving larger sample sizes (overlapping bands, where the recovery of pure product  $< 99.8\%$ ). It is therefore possible to apply our findings for isocratic separation involving larger samples (ref. 10) to corresponding separations by gradient elution.

The present study has shown that production rate in isocratic and gradient

elution is essentially the same, for the separation of a two-component mixture. Both separation procedures show production rate increasing steeply as the separation factor  $\alpha$  of the two bands (product and impurity) increases. The optimum sample size  $w/w_s$  and plate number  $N_o$  in gradient elution (for maximum production rate) is the same as for corresponding isocratic separations (Table I, Fig. 8B);  $N_o$  decreases for larger values of both sample retention ( $k'$  or  $\bar{k}$ ) and the separation factor  $\alpha$ . Once gradient and other conditions have been selected so that optimum values of  $\bar{k}$  are defined, column conditions (usually column length and flow-rate) should be varied so as to give a certain small-sample resolution:  $R_s \approx 1.6$  for the "touching-band" case, 1.2 for 95% recovery of pure product, and 0.9 for 50% recovery of pure product. Production rate increases as product recovery decreases (assumes optimized conditions), and we favor a target of 95% recovery when it is important to maximize the g/h of purified product for a column of given diameter.

Optimum values of  $k'$  and  $\bar{k}$  are somewhat different in isocratic and gradient elution, with gradient elution favoring values of  $\bar{k} > k'$ ; *i.e.*,  $3 < \bar{k} < 5$  vs.  $0.5 < k' < 2$ . Production rate in gradient elution is also influenced by the initial mobile phase, which determines the value of  $k'$  ( $k_{og}$ ) at the beginning of separation. However this dependence is not very pronounced, with  $5 < k_{og} < 100$  giving comparable production rates.

The above conclusions are strictly applicable for the usual case where the sample components (product and impurity) have a similar dependence of  $k'$  on mobile phase composition (%B); *i.e.*, the two compounds have similar  $S$  values, where  $S = -d(\log k')/d\phi$ . When the  $S$ -values of the two compounds are significantly different (by more than 2%), then the amount of sample that can be purified in a given run (*i.e.*, the weight of injected sample) can change dramatically. There is also a corresponding effect on the best choice of experimental conditions, and the results presented here can serve to guide the chromatographer in selecting the most favorable conditions for a given sample, so as to maximize production rate. For this reason, it is important to measure values of  $S$  for the sample to be separated.

The case where the composition of the feed varies was also examined, with two conclusions. First, as feed purity increases, the amount of sample that can be injected (*e.g.*, for 95% recovery of 99%-pure product) increases by 4-fold or more. Second, when an impurity is present in the feed at less than 15% of the product concentration, the fractional removal of the impurity during separation does not change for feeds containing different concentrations of the impurity relative to the product (*e.g.*, 0–15% impurity). This conclusion can be useful in fine-tuning separation conditions for maximum throughput, when the feed composition varies from batch to batch.

#### SYMBOLS

$b$	gradient steepness parameter (eqns. 1 and 2)
$k'$	solute capacity factor (usually for a small sample)
$\bar{k}$	average value of $k'$ in gradient elution
$k_{og}$	value of $k'$ at the beginning of separation (in gradient elution)
$k_x, k_y$	values of $k'$ for solutes X and Y
$n_c$	number of stages used in Craig simulation
$N_o$	column plate number, equal to $[(\bar{k} + 1)/\bar{k}] n_c$ for Craig simulation

$P_R$	production rate (arbitrary units); equal to weight of purified product produced per unit time (assumes column of fixed diameter)
$S$	solute parameter equal to $-d(\log k')/d\phi$
$S_x, S_y$	value of $S$ for solutes X and Y
$t_G$	gradient time (min)
$V_m$	column dead-volume (ml)
$w$	total sample weight injected (g)
$w_s$	column saturation capacity (g)
$w_{sx}, w_{sy}$	value of $w_s$ for X or Y (g)
$w_x, w_y$	injected weight of compounds X or Y (g)
$w_{xs}, w_{ys}$	weight of X or Y in the stationary phase (g)
X, Y	compounds to be separated (X elutes first; Y is usually the product)
$\alpha$	separation factor
$\Delta\phi$	change in $\phi$ during a gradient separation
$\phi$	mobile-phase composition; volume fraction of B solvent in a binary mobile phase A-B
$\phi_0$	value of $\phi$ at the beginning of a gradient separation

## REFERENCES

- 1 L. R. Snyder, G. B. Cox and P. E. Antle, *J. Chromatogr.*, **444** (1988) 303.
- 2 G. B. Cox, P. E. Antle and L. R. Snyder, *J. Chromatogr.*, **444** (1988) 325.
- 3 G. B. Cox, L. R. Snyder and J. W. Dolan, *J. Chromatogr.*, **484** (1989) 409.
- 4 L. R. Snyder, J. W. Dolan, D. C. Lommen and G. B. Cox, *J. Chromatogr.*, **484** (1989) 425.
- 5 L. R. Snyder, J. W. Dolan and G. B. Cox, *J. Chromatogr.*, **484** (1989) 425.
- 6 F. D. Antia and Cs. Horvath, *J. Chromatogr.*, **484** (1989) 1.
- 7 L. R. Snyder, in Cs. Horváth (Editor), *High-performance Liquid Chromatography —Advances and Perspectives*, Vol. 1, Academic Press, New York, 1986, p. 207.
- 8 L. R. Snyder and M. A. Stadalius, in Cs. Horváth (Editor), *High-performance Liquid Chromatography —Advances and Perspectives*, Vol. 4, Academic Press, New York, 1986, p. 195.
- 9 J. E. Eble, R. L. Grob, P. E. Antle and L. R. Snyder, *J. Chromatogr.*, **405** (1987) 51.
- 10 L. R. Snyder, J. W. Dolan and G. B. Cox, *J. Chromatogr.*, **483** (1989) 63.
- 11 L. R. Snyder, *J. Chromatogr.*, in press.
- 12 J. H. Knox and H. M. Pyper, *J. Chromatogr.*, **363** (1986) 1.
- 13 L. R. Snyder, G. B. Cox and P. E. Antle, *Chromatographia*, **24** (1987) 82.
- 14 M. Kunitani, D. Johnson and L. R. Snyder, *J. Chromatogr.*, **371** (1986) 313.
- 15 J. H. Knox and H. M. Pyper, *J. Chromatogr.*, **363** (1986) 1.
- 16 M. A. Quarry, R. L. Grob and L. R. Snyder, *Anal. Chem.*, **58** (1986) 907.
- 17 N. T. Miller and B. L. Karger, *J. Chromatogr.*, **326** (1985) 45.